

# A Model for Bomblet Ejection from Missiles

Raymond Sedney\*

*U.S. Army Ballistic Research Laboratory, Aberdeen Proving Ground, Md.*

Ejection of bomblets from a missile which does not have an active ejector mechanism is studied. A model is developed for this process which yields a measure of ejection time, bomblet position at early times, and trajectories. The model involves centrifugal (roll rate effect) and aerodynamic forces. A gross knowledge of the flowfield is necessary and an estimate for forces on a bomblet, while it is penetrating a shear layer, is crucial. It is shown that a bomblet may be trapped in a separated flow pocket. Results from the model are consistent with some observations and have been useful in design and performance studies.

## Nomenclature

$a$	=initial radial coordinate of bomblet center of mass, m
$A$	=cross-sectional area of bomblet or missile, $m^2$
$C_D$	=drag coefficient
$C_l$	=constant in equation preceding Eq. (5) $= a^2 \omega$
$d$	=diameter of bomblet, m
$F_s, F_n$	=forces perpendicular and parallel to shear layer, N
$F_{sm}, F_{nh}$	= $F_s, F_n$ , respectively, at that position where the bomblet center is on the vortex sheet, N
$F_x, F_r, F_\phi$	=components of applied force in cylindrical coordinates, N
$m$	=mass of bomblet, kg
$M$	=Mach number outside vortex sheet
$M_\infty$	=freestream (or missile) Mach number
$p$	=pressure at the vortex sheet, MPa
$p_\infty$	=freestream pressure, MPa
$q$	=dynamic pressure, MPa, $= \frac{1}{2} \rho_\infty V_\infty^2$
$r_0$	= $r$ -coordinate of the center of mass of the bomblet when it is tangent to the shear layer, m
$s, n$	=coordinates perpendicular and parallel to the shear layer, m
$t$	=time, s, ms
$t_e$	=ejection time, s, ms
$t_i$	=time it takes the bomblet to move up to the shear layer, s, ms
$V$	=velocity external to the vortex sheet, m/s
$V_\infty$	=freestream velocity or missile velocity at event, m/s
$W$	=weight of bomblet or missile, N
$x, r, \phi$	=cylindrical polar coordinates fixed with respect to the missile, m
$x_0$	=initial axial coordinate of the bomblet center of mass, m
$\rho_\infty$	=atmospheric density at event height, $kg/m^3$
$\omega$	=roll rate, rad/s
$\theta_s$	=shear layer angle with respect to the $x$ axis
$\Omega$	=roll rate, rev/s
$\Omega_l$	=asymptotic value of roll rate, rev/s
$(\cdot)$	=differentiation with respect to time, $d/dt$

## I. Introduction

SOME missiles have warheads which carry a large number of bomblets as payload. These are deployed at a predetermined altitude and dispersed over a wide area. The bomblets are designed to have self-induced spin which generates a Magnus-type lift; they are often called Magnus rotors. The spin also arms the fuze so that the bomblet is prepared to explode on impact. A variety of factors could interfere with the arming process. Among these is the process by which the bomblets are separated from the warhead and propelled into the freestream where they acquire their full spin. This process, called bomblet ejection, establishes the initial conditions for the subsequent flight.

The specific missile and warhead considered in analyzing ejection is the Lance with its M251 warhead. It carries about 800 bomblets which are essentially spheres (typically, diameter = 0.0572 m) with ridges to impart spin. They are deployed at low supersonic or high subsonic missile speeds after line charges cut the missile skin into two panels. In older designs, an active ejection system was used; e.g., "slings," activated by the line charges, propelled the bomblets away from the missile. In more recent designs, an active ejector is not employed, but the bomblets are usually ejected successfully. However, the governing physical process was not understood.

The purpose of this paper is to construct a model of the bomblet ejection process. A model of the process is constructed, rather than a physical description from first principles, because there are not enough data for the latter. It is specifically intended for small times; i.e., when the radial displacement of the bomblets is of the order of  $10d$ , where  $d$  is the bomblet diameter or one missile diameter. The model has proven useful in the explanation of certain anomalies in the performance of the warhead.

Several possible mechanisms for ejection are examined: inertia forces, forces due to explosive line charges, pitching motion of the missile, and the roll rate of the missile. The last of these is found to be dominant. The important elements of the model are: the flowfield after the panels have cleared the missile, the restraining force on the bomblet (which introduces the dynamic pressure) as it crosses a shear layer, and the roll rate of the missile. A straightforward calculation gives the ejection time as a function of roll rate, flowfield, restraining force, and bomblet position. Despite a number of simplifications, it is felt that the essential features of the ejection process are modeled correctly.

An important conclusion is that the time for ejection is a sensitive function of roll rate for the range of rates used in practice. The time for ejection can become infinite for small roll rates, which implies that the bomblet is trapped in a pocket of separated flow. In reality, this means ejection is

Presented as Paper 77-1164 at the AIAA 4th Atmospheric Flight Mechanics Conference, Hollywood, Fla., Aug. 8-10, 1977; submitted Oct. 7, 1977; revision received April 3, 1978. Copyright © American Institute of Aeronautics and Astronautics, Inc., 1977. All rights reserved.

Index categories: Jets, Wakes, and Viscid-Inviscid Flow Interactions; LV/M Aerodynamics; Missile Systems.

\*Research Physicist. Member AIAA.

delayed; the bomblets eventually clear the missile, at times so large that the model no longer applies. As the roll rate approaches zero, the model predicts large ejection times for all bomblets. The basis for the model no longer exists, since the effects which were negligible must become dominant if the roll rate goes to zero. An alternate model, not considered here, was developed which would give ejection even for zero roll rate; the results were quite different from those of the first model.

For system performance studies, a knowledge of bomblet ejection is useful in two ways. The model can give initial conditions for a detailed study of bomblet trajectories and spin. Rather than a deterministic approach, a statistical one can be used. The function of the model is then to provide correlation parameters; this will be discussed in a separate report. Its success provides some indirect, partial support for the validity of the model.

The only data available to evaluate the model are the time of appearance and the shape of the distribution of the bomblets as determined from a few film records. It is difficult to obtain accurate readings from these records but they show that, typically, the bomblets first appear at 100 ms, at which time they are about 0.61 m from the missile. Results from the model are in general agreement with these observations. In one case the film records were clear enough to measure the shape of the distribution of bomblets. The calculated results are consistent with the measurement. Thus, some basis for confidence in the model exists; no more than that can be said, at present.

## II. Bomblet Ejection Model

There are three items to consider: 1) the forces acting on the bomblets other than the flowfield forces, 2) the flowfield, and 3) the force on a bomblet as it penetrates the shear layer.

The packing of the bomblets in the warhead must be discussed first. From the manner in which they are packed, the initial distribution of bomblets will vary with each warhead. Figure 1 shows an ideal distribution which gives the correct total number of bomblets; three rows are shown and the bomblets are numbered for later reference. In practice, the bomblets are not necessarily loaded in such a regular pattern and distribution would be somewhat different but unknown. A choice of initial positions must be made, however, and the one shown in Fig. 1 is convenient for calculations. The skin and nose are shown by dashed lines. At "event time," the skin panels and nose are blown off leaving the configuration shown by the solid lines.

The missile flies at a small angle of attack with a nominal roll rate of 5 rev/s. Only supersonic flight at event time is considered. It takes about 10 ms for the panels to lift off and about 50 ms to complete the separation process. The fuze ring and pedestal may or may not be lost at early times. After the panels and nose are removed a new flowfield is established. From the correlations given in Ref. 1, about 10 ms are required to establish the flow with the fuze ring in place and probably about the same without the fuze ring. A typical time

of 10 ms will be used in the discussion of the forces that were examined vis-à-vis ejection. The parameters for a specific Lance flight will be used in making the following estimates.

### A. Forces on the Bomblets, Excluding Flowfield Forces

Immediately after skin release the forces are:

1) An inertia force which tends to move the bomblets to the front. This is caused by the sudden change in drag coefficient,  $\Delta C_D$ , because the low drag nose is ejected. An adequate approximation is  $\Delta C_D = 1.0$ . The axial acceleration of the bomblets with respect to the missile is then  $47.5 \text{ m/s}^2$ . In 10 ms the bomblets are displayed axially 0.0023 m. This effect will be neglected.

2) Forces due to the line charge. Blast and detonation waves cause an impulsive force. The pressures are several MPa's, but act only near the charge and last for about  $10 \mu\text{s}$ . This can be neglected. From the burning of detonation products there will be a residual pressure in the warhead volume, estimated to be 2.07 MPa. This is relieved by an expansion wave propagating in from the moving panels; while the wave traverses a bomblet, an outward radial force acts on it. A rough model of this effect gives a maximum acceleration of  $97.5 \text{ m/s}^2$  in a radial direction. In 10 ms the bomblet would move 0.0048 m if the acceleration were constant; but it lasts for about 1 ms. Therefore, this will be neglected.

3) Pitching moment of the missile. When the nose and skin panels are removed, forces act on the missile that cause pitching motion. With respect to the missile, some bomblets will accelerate in a direction normal to the missile axis. The information necessary to calculate the magnitude of this effect was not available. However, some estimates of it were made. In the first quarter-cycle, which lasts about 170 ms, bomblets on the windward side are displaced radially, whereas those on the leeward side are not displaced until the second quarter-cycle. Photographs of a number of flights, including subsonic and supersonic cases, show that the time for the bomblets to move about 1 missile diameter (about 0.61 m for the Lance) ranges from 80 to 130 ms. Based on these times, this mechanism does not seem plausible; nor does it from an estimate of displacements. If no other forces act, in 10 ms bomblet 1a (Fig. 1), has a significant displacement, about 0.02 m, but bomblets 28a or 7c would be displaced 0.002 m, which is negligible. This implies that the aggregate of bomblets tips during ejection; there is no evidence for this. Although it has not been established that this mechanism can be neglected, it is much less plausible than the roll rate effect and, therefore, will not be considered further.

4) Release of centrifugal constraint. The nominal roll rate is 5 rev/s. When the skin is removed the bomblets will move tangentially in a straight line at constant velocity if there are no other forces acting on the bomblet (see Fig. 2a). For the inner row, a in Fig. 1, with the diameter of the central tube being 0.178 m, the initial acceleration is  $116 \text{ m/s}^2$  (11.8 g), the initial velocity is 3.69 m/s and in 10 ms a bomblet would be displaced radially 0.0056 m. The same quantities for the outer row, c, are:  $229 \text{ m/s}^2$  (23.3 g), 7.28 m/s, and 0.011 m. For the

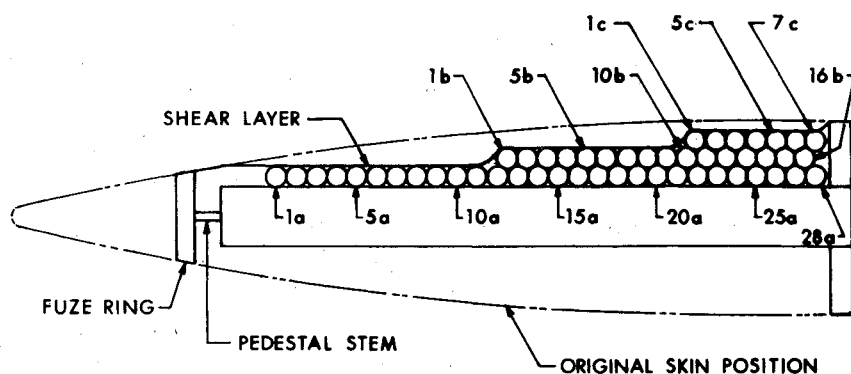


Fig. 1 Sketch of a missile warhead containing an idealized packing of bomblets in three rows (a, b, and c). The shear layer is formed after the dashed line configuration is removed.

case of no forces, the radial motion is obtained from a simple calculation. The distance,  $r(t)$ , from the missile axis to the bomblet center, at time  $t$ , is given by

$$r = a / \cos(\tan^{-1} 2\pi\Omega t) \quad (1)$$

where  $a = r(0)$  and  $\Omega$  is the roll rate in rev/s. Actually, there are forces, described in Sec. B, that may even prevent the bomblet from being ejected at early times. These forces are an important part of the model, but if they are neglected for the moment, Eq. (1) gives, for  $\Omega = 5$  rev/s, radial positions at  $t = 100$  ms of 0.396, 0.579, and 0.762 m for rows a, b, and c, respectively. These radial distances are in the neighborhood of those observed. Of course the bomblet distribution will not be correct because the other forces have been neglected, but even this overly simplified approach gives reasonable results. Release of the centrifugal constraint is the most plausible mechanism for bomblet ejection; it will now be incorporated into a model.

The spin of the bomblets and the ridges which cause it are ignored; they are treated as spheres with diameter  $d = 0.0572$  m. Only the motion of the center of mass of the bomblets will be described. The equations of motion are written in a cylindrical polar coordinate system fixed with respect to the missile. Since the missile decelerates, this is not an inertial system. However, the axial deceleration is 1/14 that of a bomblet (or  $W/C_D A$  is 14 times greater) and will be neglected. For an inertial system, with  $x$  the axial coordinate along the centerline of the missile and  $r$  and  $\phi$  polar coordinates in the plane  $x = \text{constant}$ , the equations of motion are

$$m(\ddot{r} - r\dot{\phi}^2) = F_r \quad (2)$$

$$mr^{-1}d(r^2\dot{\phi})/dt = F_\phi = 0 \quad (3)$$

$$m\ddot{x} = F_x \quad (4)$$

with initial conditions at  $t = 0$  when the flow is first established

$$r = a \quad \dot{r} = 0$$

$$\phi = 0 \quad \dot{\phi} = a\omega$$

$$x = x_0 \quad \dot{x} = 0$$

Here,  $m$  is the mass, 0.419 kg, of the bomblet,  $x_0$  and  $a$  are the initial axial and radial coordinates of the bomblet,  $\omega$  is the roll rate in rad/s, and the applied forces are  $F_r$ ,  $F_\phi$ ,  $F_x$ . Assuming axial symmetry, there is no force in the  $\phi$  direction and Eq. (3) can be integrated, giving

$$r^2\dot{\phi} = C_I = a^2\omega$$

This equation is not integrated since the circumferential motion is not needed in the model. It is used to simplify Eq. (2). Thus, the equations to be integrated are

$$\ddot{r} = C_I^2/r^3 + F_r/m \quad (5)$$

$$\ddot{x} = F_x/m \quad (6)$$

The term  $C_I^2/r^3$  is the apparent centrifugal force which accelerates the bomblet even if there is no force; i.e., if  $F_r = 0$ . In that case, Eq. (1) can be derived from Eq. (5); but this is the hard way to do it. If  $F_r$  and  $F_x$  are functions of  $r$  only the equations can be integrated by quadrature after using the substitutions  $2\dot{r} = d^2r/dt^2$  and  $\ddot{x} = r d\dot{x}/dr$ . In general,  $F_r$  and  $F_x$  are functions of both  $r$  and  $x$ , so that a numerical integration is required.

## B. Flowfield

Although some parts of the flowfield will certainly be unsteady, we shall assume steady flow here. (There are some

analogies with flow over a spiked-nose projectile which are useful in thinking about the flowfield.) For the kind of bomblet distribution shown in Fig. 1, the steady flow near the bomblets would have regions of attached and separated flow. Some schlieren pictures of the flow over a configuration similar to that of Fig. 1 were available (Ref. 2) and were used as a guide for approximating the flowfield. The shear layer indicated in Fig. 1 is drawn with the help of those pictures. The shear layer angle with respect to the  $x$  axis,  $\theta_s$ , varies between 0 and 20 deg. Actually, slightly negative values are possible and the pictures of Ref. 2 can be interpreted to give  $\theta_s = 25$  deg. At  $t = 0$ , most of the bomblets will be encased in the shear layer, but the flow will attach on some of them; these will be subject to an additional force not considered in the next paragraph. Calculations have been made for a range of values of  $\theta_s$  and for a bomblet on which the flow attaches. The shear layer is important because, until they penetrate it, the bomblets are shielded by it from the flow outside the shear layer which has high dynamic pressure,  $q$ . This external flow could be obtained from a calculation of the inviscid flow over the fuze ring and shear layer. Such sophistication is unwarranted; the flow variables immediately outside the shear layer were obtained from the flow over a flat-faced cylinder. Inside the shear layer,  $q$  and the aerodynamic forces are small. In Fig. 2b two typical bomblets which have moved from their original position are shown. The only significant force acting on them until they reach the shear layer is the centrifugal force. The question then is: can a bomblet penetrate the shear layer?

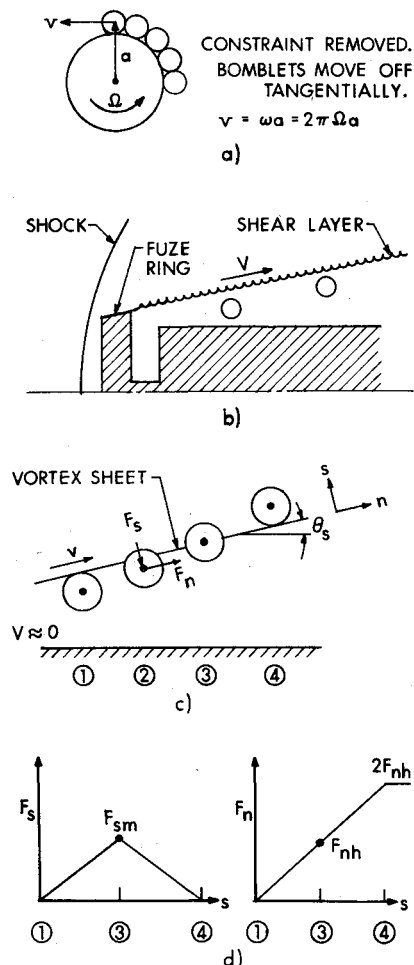


Fig. 2 The elements of the bomblet ejection model: a) a cross-sectional view of some bomblets on the central tube after release of the centrifugal constraint; b) two typical bomblets moving toward the shear layer, with only centrifugal force acting; c) bomblet penetration of the vortex sheet; d) assumed force distribution.

### C. Model for Penetration of the Shear Layer by a Bomblet

The complicated interaction between a bomblet and the shear layer flow must be modeled in a simple way that retains the essence of the process. Specifically, an approximation to the forces on the bomblet is needed. Three assumptions are made for this purpose. First, the shear layer is replaced by a vortex sheet; i.e., an inviscid shear layer. Second, the shear layer remains fixed while a bomblet penetrates it. These are illustrated in Fig. 2c; the small velocity inside the shear layer is taken to be zero. Let the components of the force on the bomblet, parallel and perpendicular to the shear layer, be  $F_s$  and  $F_n$ ; the latter is called the restraining force. In principle, we could calculate the force on the bomblet as it passes through the vortex sheet, treating the flow as inviscid and quasisteady. But the flow over a segment of a bomblet, position 2 in Fig. 2c, is three-dimensional and such an elaborate calculation is unjustified and unacceptable for our purpose. There is one position of the bomblet where the calculation becomes simple, viz., that for which the bomblet center is on the vortex sheet, position 3 in Fig. 2c. Then we have flow over a hemisphere. For this position we denote  $F_s$  and  $F_n$  by  $F_{sm}$  and  $F_{nh}$ , respectively. Experimentally determined pressure distributions over a sphere can be used to calculate  $F_{sm}$  and  $F_{nh}$ . The data of Ref. 3 were used since they were particularly well suited for this purpose. The freestream (or missile) Mach number is  $M_\infty = 1.82$  for a typical flight for which results will be presented. Then  $p = 0.5 p_\infty$  and  $M = 2.13$ , where  $p$  and  $M$  are the pressure and Mach number outside the vortex sheet at the position of bomblet 1a. Using the procedure just outlined we obtain  $F_{sm} = 22.2$  N and  $F_{nh} = 200$  N. As a check on the calculation, note that  $2F_{nh} = 400$  N is within a few percent of the drag force obtained from the standard  $C_D$  for a smooth sphere. Because of the ridges on the bomblet,  $F_{sm}$  and  $F_{nh}$  will be larger than the results for a smooth sphere; the magnitude of the increase depends on the orientation of the bomblet. The third assumption is that the forces are taken to be linear functions of  $s$ , the distance of the bomblet across the shear layer and, in position 4,  $F_s = 0$  and  $F_n = \text{drag of a sphere}$ . The resulting force distributions are illustrated in Fig. 2d. Some obvious refinements to these force distributions could be made but, because of uncertainties in the physical processes we are trying to analyze and in other elements of the model, this is not justified in a first approximation. The forces that enter Eqs. (5) and (6) are then

$$F_r(s) = -F_s(s) \cos\theta_s + F_n(s) \sin\theta_s \quad (7)$$

$$F_x(s) = F_s(s) \sin\theta_s + F_n(s) \cos\theta_s \quad (8)$$

where

$$s = (r - r_0) \cos\theta_s - (x - x_0) \sin\theta_s$$

and  $r_0$  is the  $r$  coordinate of the center of the bomblet when it is tangent to the shear layer, as in position 1 in Fig. 2c. Each  $F$  in Eqs. (7) and (8) is a linear function of  $s$ , or constant; they are zero for  $s \leq 0$ . The bomblet accelerates in the  $r$  direction under the influence of centrifugal force, but its axial coordinate is fixed at  $x = x_0$  until it becomes tangent to the shear layer. It then feels the effect of both  $F_r$  and  $F_x$ . If its radial momentum plus the centrifugal effect are large enough to overcome  $F_r$ , the bomblet penetrates the shear layer and is ejected.

The motion is easily illustrated for the special case  $\theta_s = 0$  because Eq. (5) can be integrated once. Consider row a so that  $r_0 = a$  and  $s = r - a$ . Then from Fig. 2d, where  $s = d/2$  at position 3, and Eq. (7),

$$F_r = -F_s = -2F_{sm}(r - a)/d \quad \text{for } a \leq r \leq a + (d/2) \quad (9)$$

$$= -2F_{sm}[d - (r - a)]/d \quad \text{for } a + (d/2) \leq r \leq a + d \quad (10)$$

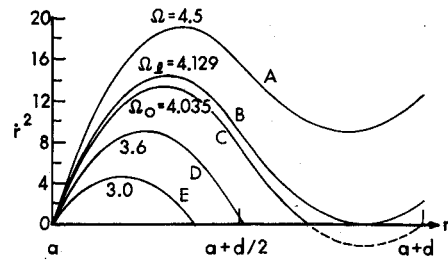


Fig. 3 Phase plane diagram,  $r^2$  vs  $r$ , of the motion of a bomblet in row a for  $\theta_s = 0$ ,  $F_{sm} = 35.6$  N (8 lbf),  $m = 0.419$  kg (0.0287 slugs),  $a = 0.117$  m,  $d = 0.0572$  m, and  $\Omega$  (rev/s) as a parameter.

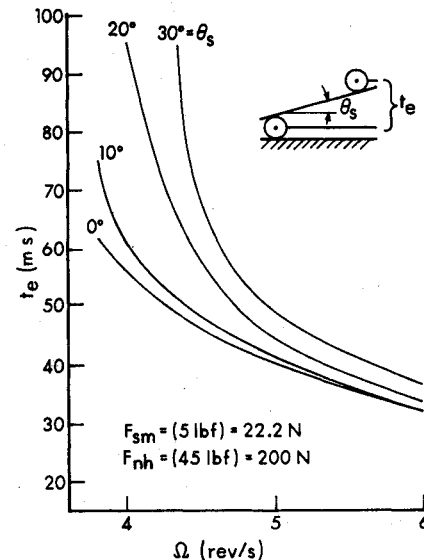


Fig. 4 For bomblet 1a, ejection time vs roll rate with shear layer angle as the parameter.

Using these and  $2\ddot{r} = d\dot{r}^2/dr$  in Eq. (5) yields

$$\dot{r}^2 = a^4 \omega^2 (a^{-2} - r^{-2}) - 2F_{sm}(r - a)^2/md \quad (11)$$

and

$$\dot{r}^2 = a^4 \omega^2 (a^{-2} - r^{-2}) + [d^2 - 4d(r - a) + (r - a)^2] F_{sm}/md \quad (12)$$

for the two ranges of  $r$  given in Eqs. (9) and (10), respectively. For the values of the parameters  $a = 0.117$  m,  $d = 0.0572$  m,  $m = 0.419$  kg, and using  $F_{sm} = 35.6$  N,  $\dot{r}$  vs  $r$  is plotted in Fig. 3 for various  $\Omega = \omega/2\pi$ ;  $t$  is a parameter along each curve with  $t = 0$  at  $r = a$ . The bomblet penetrates the shear layer for  $\Omega = 4.5$  rev/s, curve A, but does not for any of the other curves. As  $\Omega$  decreases the bomblet continues to escape, but the time to do so increases until a limiting value,  $\Omega_l$ , is reached; here  $\Omega_l = 4.129$  rev/s. For this curve B, Eq. (12) has a double root and the time to reach that value of  $r$  is infinite. For curves C, D, and E the bomblet would oscillate between  $r = a$  and the other for which  $\dot{r} = 0$ , according to this idealized model.

In summary, after the bomblets have been exposed and the flow established, the forces are defined by a knowledge of the shear layer, the inviscid flow outside the shear layer, and the forces acting on a hemisphere at the local flow conditions. The magnitude of these forces depends on the dynamic pressure. Since it is expected that this model will yield only estimates or be used for comparative purposes, a precise knowledge of the flowfield is not necessary. For example, if the missile is at angle of attack, the angle and position of the

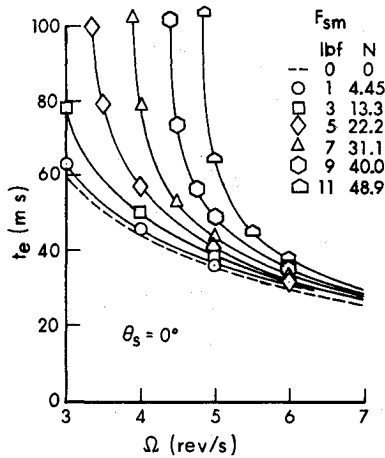


Fig. 5 For all bomblets in row a, ejection time vs roll rate with restraining force as parameter.

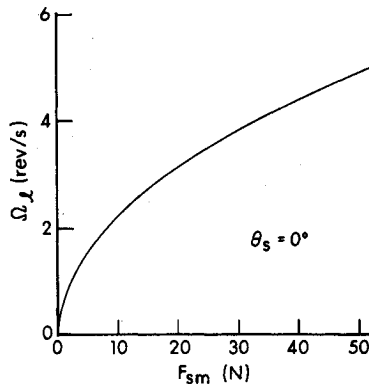


Fig. 6 The limiting roll rate at which  $t_e \rightarrow \infty$  for all bomblets in row a vs the restraining force.

shear layer can be estimated from wind-tunnel or ballistic range shadowgraphs of configurations that approximate the warhead plus bomblets. In any case, to obtain useful results, the parameters will have to be varied from their initial estimates because of the number of simplifying assumptions incorporated in the model.

### III. Results

The model was used to calculate some results pertinent to ejection for a typical supersonic flight of the Lance. The velocity at event time is taken as 609.6 m/s ( $M_\infty = 1.82$ ) and zero angle of attack is assumed. The input quantities are  $x_0$ ,  $a$ ,  $\theta_s$ ,  $F_{sm}$ ,  $F_{nh}$ , and the roll rate in rev/s,  $\Omega$ . In Fig. 1,  $\theta_s$  varies between 0 and 20 deg. To simplify matters, the results are presented for a constant  $\theta_s$  for all bomblets or for one specific bomblet. It is more tedious to do the calculations using the  $\theta_s$  corresponding to each bomblet. Of course, as the bomblets penetrate the shear layer,  $\theta_s$  changes. This interaction and that of one bomblet with another are neglected; the motion of each bomblet is treated without regard to another. Note that, for a constant  $\theta_s = 5$  deg, the shear layer would be a straight line joining the fuze ring and the rear wall of the cargo compartment.

The model should answer the questions: will the bomblets penetrate the shear layer and, if so, how long will it take? The ejection time,  $t_e$ , is defined as the time for a bomblet to be displaced radially one diameter across the shear layer; it is the time between positions 1 and 4 in Fig. 2c and is also indicated in Fig. 4.

For bomblet 1a (see Fig. 1)  $t_e$  vs  $\Omega$  for various  $\theta_s$  is presented in Fig. 4. For smaller  $\Omega$ ,  $t_e$  is a sensitive function of  $\theta_s$ . In fact each curve has an asymptote for some  $\Omega$ ; i.e.,

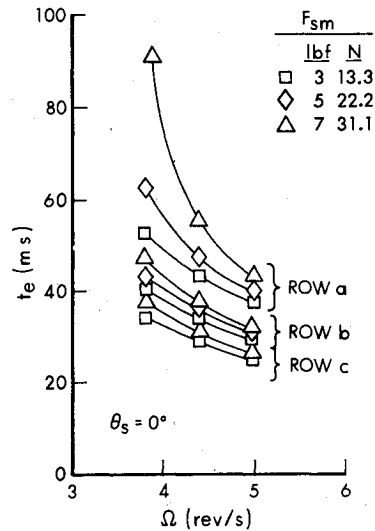


Fig. 7 For all bomblets in rows a, b, and c, ejection time vs roll rate with restraining force as parameter.

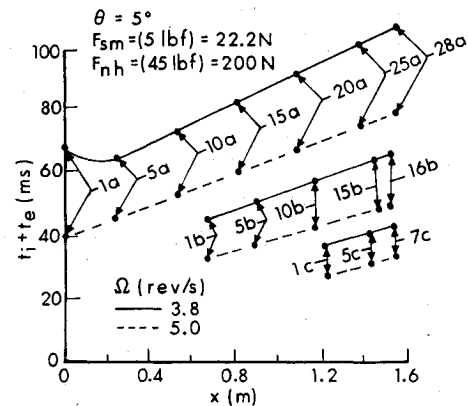


Fig. 8 The total time for each bomblet to get across the shear layer vs its axial coordinate at  $t = 0$ , for two roll rates.

$t_e \rightarrow \infty$ , which means the bomblet never penetrates the shear layer, it is trapped under the shear layer. Figure 5 applies to all bomblets in row a and shows  $t_e$  vs  $\Omega$  for  $\theta_s = 0$  for a range of  $F_{sm}$  above and below the value of 22.2 N derived in the last section for a smooth sphere.  $F_{sm} = 0$  implies  $F_r = 0$  which was discussed in Sec. 2; the motion is determined by Eq. (1) which also gives the equation of the dashed curve in Fig. 4:

$$2\pi\Omega t_e = \tan[\cos^{-1}(a/\{a+d\})]$$

This has an asymptote at  $\Omega = 0$ . For each  $F_{sm}$  there is an asymptote at  $\Omega = \Omega_L$ ; the relationship between  $\Omega_L$  and  $F_{sm}$  is shown in Fig. 6 for  $\theta_s = 0$ . For comparison, the values for two other  $\theta_s$  are given: for  $\theta_s = 10$  deg,  $\Omega_L = 3.8$  rev/s and  $F_{sm} = 23.8$  N and for  $\theta_s = 30$  deg,  $\Omega_L = 4.3$  rev/s and  $F_{sm} = 22.2$  N. The asymptote is easily explained physically. If the radial momentum plus the centrifugal effect are large enough to overcome the radial component of force, the bomblet is ejected; i.e.,  $t_e$  is finite. When these just balance,  $t_e \rightarrow \infty$ . Thus, decreasing  $\Omega$ , increasing  $F_{sm}$ , or increasing  $\theta_s$  will force the bomblet back into the shear layer and it will not be ejected; this behavior is shown in computed trajectories. The correct interpretation of this result is that the ejection time becomes large, by which time the angle of attack of the missile is so large that the model can no longer be used without modification.

Trapping of a bomblet and the existence of  $\Omega_L$  was explained earlier using Fig. 5 for the special case  $\theta_s = 0$ . In principle,  $\Omega_L$  can be found by determining the  $\Omega$  for which Eq.

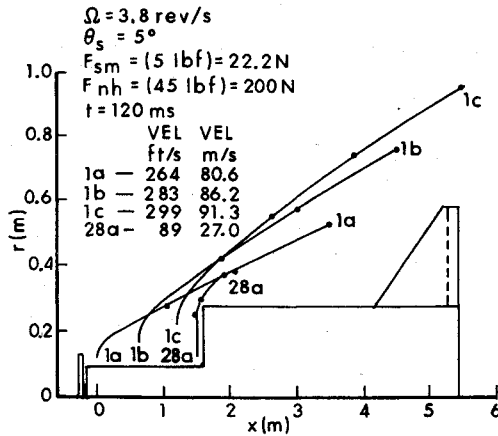


Fig. 9 Trajectories for bomblets 1a, 1b, 1c, and 28a and their velocity at  $t = 120$  ms. The three dots on each trajectory are at  $t = 80$ , 100, and 120 ms.

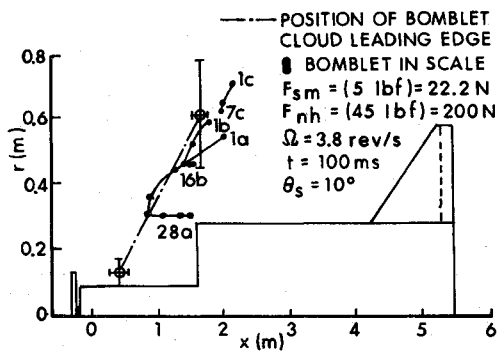


Fig. 10 The solid curves through the dots give the distribution at  $t = 100$  ms of the bomblets initially in rows a, b, and c. The significance of the dots is given in the text. The dashed line is obtained from a test result.

(12) has double roots. Since the roots of a quartic must be found, a convenient general expression for  $\Omega_l(F_{sm})$  cannot be given; however, it is obvious from Eq. (12) that  $\Omega_l \propto F_{sm}^{1/2}$ . A convenient expression for  $\Omega_0(F_{sm})$  can be found where  $\Omega_0$  is determined from  $\dot{r} = 0$  at  $r = a + d$ ; see curve C in Fig. 3, for which the dashed portion has no physical meaning. The result is

$$\Omega_0^2 = (a + d)^2 F_{sm} / 4\pi^2 a^2 m (2a + d)$$

Since  $\Omega_0$  is within a few percent of  $\Omega_l$ , this expression is adequate considering the approximate nature of the model.

The sensitivity of  $t_e$  to  $\Omega$ , for a given  $F_{sm}$ , is not the same for all bomblets, even for a constant  $\theta_s$ . Figure 7 shows  $t_e$  vs  $\Omega$  for rows a, b, and c of Fig. 1. Because  $\theta_s = 0$ ,  $t_e$  is the same for all bomblets in a row. The results for row a (already given in Fig. 5) show that  $t_e$  for these bomblets is more sensitive to decreasing  $\Omega$  than it is for rows b and c. This is because the centrifugal force acting on them, through the factor  $C_l$  in Eq. (5), is greater.

The definition of  $t_e$  does not account for the time it takes for a bomblet to move up to the shear layer,  $t_i$ , which can be obtained from Eq. (1). The total time for a bomblet to get across the shear layer is  $t_i + t_e$ . This is shown in Fig. 8 for  $\theta_s = 5$  deg,  $F_{sm} = 22.2$  N and two roll rates, 3.8 and 5.0 rev/s. For the 3.8 case, the two times for bomblet 28a are  $t_i = 79.7$  ms and  $t_e = 26$  ms; for bomblet 1a,  $t_i = 0$  and  $t_e = 66.6$  ms.  $t_e$  is smaller for bomblet 28a because of its greater momentum when it reaches the shear layer. The non-monotonic behavior for row a with  $\Omega = 3.8$  rev/s is an indication that the first few bomblets are close to the asymptote.

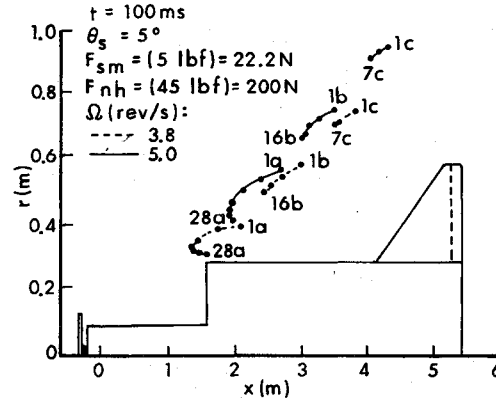


Fig. 11 The distribution at  $t = 100$  ms of the bomblets initially in rows a, b, and c for two roll rates. The significance of the dots is the same as in Fig. 9.

A knowledge of  $t_e$  and  $t_i$  are useful in design and performance studies and the existence of the asymptote is an important result from the model. Considering the various  $\theta_s$  appropriate to the bomblets, we can conclude that only a fraction of the bomblets would be trapped for certain  $\Omega$  and  $F_{sm}$ .

Trajectories for bomblets 1a, 1b, 1c, and 28a are shown in Fig. 9 with  $\Omega = 3.8$  rev/s and  $\theta_s = 5$  deg; the velocities, relative to the missile, at  $t = 120$  ms are also listed. Note the different scales in the axial and radial directions. After ejection, the point mass trajectories are computed with  $F_s = 0$  and  $F_n = 2F_{nh}$ , which means that the direction of the force is fixed at an angle  $\theta_s$  with respect to the missile axis. The lift on a bomblet is neglected. The three dots on each trajectory locate  $t = 80$ , 100, and 120 ms. There are some obvious uses for the trajectories; e.g., determining if a control surface is struck by a bomblet.

The distribution of all bomblets at  $t = 100$  ms is shown in Fig. 10 for  $\Omega = 3.8$  rev/s and  $F_{sm} = 22.2$  N. The shear layer angle was taken to be constant;  $\theta_s = 10$  deg was chosen to give the best agreement with a test result discussed later. The positions of rows a, b, and c are shown by curves; the first and last bomblets in each row are indicated by a dot and are numbered; the other dots show the positions of bomblets whose number is a multiple of 5. The spherical bomblet appears to be elliptical because of the different  $x$  and  $r$  scales. The distribution shows that some bomblets would have collided, an effect which is neglected. For a test in which  $\Omega = 3.8$  rev/s, the bomblets could be discerned in a photograph from the ground taken at  $t = 100$  ms; the bomblets appear as a dark cloud near the missile. The leading edge of this cloud is shown in Fig. 10 as a dashed straight line connecting the two ends points which have error bars attached. The quality of the photograph did not permit a more accurate measurement. The perspective of the photograph does not allow the distribution of bomblets to be determined, but the leading edge can be compared with the front of the calculated distribution. The agreement between these is close enough to give confidence in the model.

The effect on the distribution of changing  $\Omega$  is shown in Fig. 11. As expected, the radial displacement of the bomblets is greater for the larger  $\Omega$ ; the axial displacement is also increased. For  $\Omega < 3.8$  rev/s, some of the bomblets would not appear in the distribution since they would have been trapped by the shear layer.

#### IV. Conclusions

The problem of bomblet ejection from missiles which do not have an active ejection system has been studied. A model was formulated for the ejection process, the crucial elements of which are the centrifugal effect due to the spin of the

missile and the interaction of the bomblets with the shear layer. An ejection time is defined which can be used as a measure of the effect of various parameters on the ejection process. For a given shear layer angle and restraining force, this time becomes infinite as the roll rate decreases. Taken literally, this implies that a bomblet will be trapped under the shear layer. Realistically it means that the time for ejection is large, at which time the conditions for the model's validity are not met. Such delayed ejection can affect the performance of the system. Bomblet trajectories and distributions have also been presented. In one case, the calculated distribution is compared with the shape of the distribution determined in a test. The agreement is favorable enough to lend credence to the model.

### Acknowledgments

In various aspects of this work, assistance was received from B. Bertram, W. Chase, N. Gerber, G. Kahl, C. Kit-chens, and M. Morkovin. Special thanks to J. Bartos who did all of the calculations and aided in preparing this report.

### References

- <sup>1</sup>Holden, M. S., "Establishment Time of Laminar Separated Flows," *AIAA Journal*, Vol. 9, Nov. 1971, pp. 2296-2298.
- <sup>2</sup>Loeb, A., private communication. Picatinny Arsenal, May 6, 1976.
- <sup>3</sup>Bennett, F. D., Carter, W. C., and Bergdolt, V. E., "Interferometric Analysis of Airflow About Projectiles in Free Flight," *Journal of Applied Physics*, Vol. 23, April 1952, pp. 453-469.

## *From the AIAA Progress in Astronautics and Aeronautics Series . . .*

### **TURBULENT COMBUSTION—v. 58**

*Edited by Lawrence A. Kennedy, State University of New York at Buffalo*

Practical combustion systems are almost all based on turbulent combustion, as distinct from the more elementary processes (more academically appealing) of laminar or even stationary combustion. A practical combustor, whether employed in a power generating plant, in an automobile engine, in an aircraft jet engine, or whatever, requires a large and fast mass flow or throughput in order to meet useful specifications. The impetus for the study of turbulent combustion is therefore strong.

In spite of this, our understanding of turbulent combustion processes, that is, more specifically the interplay of fast oxidative chemical reactions, strong transport fluxes of heat and mass, and intense fluid-mechanical turbulence, is still incomplete. In the last few years, two strong forces have emerged that now compel research scientists to attack the subject of turbulent combustion anew. One is the development of novel instrumental techniques that permit rather precise nonintrusive measurement of reactant concentrations, turbulent velocity fluctuations, temperatures, etc., generally by optical means using laser beams. The other is the compelling demand to solve hitherto bypassed problems such as identifying the mechanisms responsible for the production of the minor compounds labeled pollutants and discovering ways to reduce such emissions.

This new climate of research in turbulent combustion and the availability of new results led to the Symposium from which this book is derived. Anyone interested in the modern science of combustion will find this book a rewarding source of information.

485 pp., 6 × 9, illus. \$20.00 Mem. \$35.00 List

TO ORDER WRITE: Publications Dept., AIAA, 1290 Avenue of the Americas, New York, N. Y. 10019